





Communication

# A Novel Approach to Water Softening Based on Graphene Oxide-Activated Open Cell Foams

Riccardo Balzarotti <sup>1,2</sup>, Alessandro Migliavacca <sup>1,3,\*</sup>, Andrea Basso Peressut <sup>4,\*</sup>, Alessandro Mansutti <sup>1</sup>  
and Saverio Latorrata <sup>4</sup><sup>1</sup> Elettrotecnica ROLD, Via della Merlata 1, 20014 Nerviano, Italy<sup>2</sup> Department of Innovative Technologies (DTI), University of Applied Sciences and Arts of Southern Switzerland (SUPSI), 6962 Lugano, Switzerland<sup>3</sup> Department of Materials Science, University of Milano-Bicocca, Via Roberto Cozzi 55, 20125 Milan, Italy<sup>4</sup> Department of Chemistry, Materials and Chemical Engineering "Giulio Natta", Politecnico di Milano, Piazza Leonardo Da Vinci 32, 20133 Milan, Italy

\* Correspondence: alessandro.migliavacca@rold.com (A.M.); andreastefano.basso@polimi.it (A.B.P.)

**Abstract:** This work focuses on exploring a new configuration for the reduction of water hardness based on the surface modification of polyurethane (PU) open cell foams by the deposition of thin graphene oxide (GO) washcoat layers. GO was deposited by the dip-squeeze coating procedure and consolidated by thermal treatment. The final washcoat load was controlled by performing consecutive depositions, after three of which, a GO inventory up to 27 wt% was obtained onto PU foams of 60 pores per inch (PPI). The GO-coated PU foams were assembled into a filter, and the performance of the system was tested by continuously feeding water with hardness in the 190–270 mg<sub>Ca2+,eq</sub>·L<sup>-1</sup> range. Remarkable results were demonstrated in terms of total adsorbing capacity, which was evaluated by measuring the outlet total hardness by titration and exhibited values up to 63 mg<sub>Ca2+,eq</sub>·g<sub>GO</sub><sup>-1</sup> at a specific filtered water volume of 650 mL<sub>H2O</sub>·g<sub>GO</sub><sup>-1</sup>, outperforming the actual state-of-the-art adsorbing capacity of similar GO-based materials.

**Keywords:** graphene oxide; open cell polyurethane foams; washcoating; water softening; filtration

**Citation:** Balzarotti, R.; Migliavacca, A.; Basso Peressut, A.; Mansutti, A.; Latorrata, S. A Novel Approach to Water Softening Based on Graphene Oxide-Activated Open Cell Foams. *C* **2023**, *9*, 6. <https://doi.org/10.3390/c9010006>

Academic Editors: Sergey  
Mikhailovsky and Rosa Busquets

Received: 15 December 2022

Revised: 4 January 2023

Accepted: 5 January 2023

Published: 7 January 2023



**Copyright:** © 2023 by the authors. Licensee MDPI, Basel, Switzerland. This article is an open access article distributed under the terms and conditions of the Creative Commons Attribution (CC BY) license (<https://creativecommons.org/licenses/by/4.0/>).

## 1. Introduction

In recent years, graphene (G) and its derivatives, such as graphene oxide (GO) and reduced graphene oxide (rGO), have gained high visibility in research, in view of their very promising properties. Since the isolation of the material in 2004 [1], an increasing number of research reports have been published in the literature. Accordingly, a variety of reviews has been proposed, focusing on different aspects such as production [2], characterization, and potential applications [3,4]. Thanks to graphene and GO peculiar properties, these materials have found a variety of applications in processes where high water permeability, high selectivity and capability of rejecting monovalent ions, high salt rejection, reduced fouling, and high chemical and physical stability are major concerns [5]. Moreover, the possibility to produce thin membranes with controllable selectivity and high permanence has widened the investigation of nanoporous single-layer graphene and multilayer GO membranes in separation processes, enabling the potential use of GO-based materials in filtration applications in a wide variety of forms [6]. Accordingly, many efforts have been spent to test membranes based on GO precursors in several application areas, such as water purification [7], desalination [8,9], gas separation [10], organic solvent filtration [11], and energy production by proton-exchange membrane fuel cells [12–14].

In the recent literature, a comprehensive state of the art of 2D graphene-based materials has been reported. Many complete reviews are available concerning the preparation methods [15], with special attention devoted to physical fabrication methodologies and to their scalability to industrial processes [11]. In a similar way, Li et al. exhaustively

discussed the most recent findings concerning the effects on the macroscopic properties of GO membranes obtained by tailoring the properties of GO nanosheets by different approaches (e.g., chemical modification, intercalation, and crosslinking) [16]. With a similar approach, multilayered GO membranes were comprehensively reviewed by Wei et al., with a dedicated focus on preparation and performance control methods, stability, fouling resistance and applications [17].

As previously reported, the peculiar chemical and physical properties of GO have been exploited in many different applications. Among others, the selectivity towards metal ions adsorption has been investigated in self-assembling filters for wastewater treatment based on reduced graphene oxide (rGO) membranes [18]. With a similar approach, Rocha et al. explored GO materials with their surface modified by  $\kappa$ -carrageenan as a biopolymer-based softener. The experimental results evidenced a decrease of the hardness of natural waters containing high levels of  $\text{Ca}^{2+}$  ions [19]. GO membranes were found to be able to adsorb  $\text{Ca}^{2+}$  ions from hard water, with uptake values up to 0.05 mg of  $\text{Ca}^{2+}$  ions per mg of GO membrane [20].

While membranes can be effectively used in many technological fields, some intrinsic drawbacks are present, such as pressure drops and the difficulty to find reliable and cost-effective procedures for the fabrication of defect-free GO membranes on different large area substrates [5,21].

Many of the aforementioned limitations can be effectively overcome by adopting porous matrices or three-dimensional cellular structures, which are characterized by a significantly high surface area per unit volume and relatively low pressure drops, if compared to membrane-based systems [22]. In this view, hollow fibers represent a possible solution to enhance the performance in nanofiltration separation. Mahalingam et al. reported the production of hollow fibers made of polyetherimide, which were spray-coated from GO dispersions using an air brush [23]. The as-prepared samples were effectively tested towards organic solvent nanofiltration. Recently, Maio et al. developed a one-pot process for decorating either pearl necklace-like or fibrous fluffy-like structures of polycaprolactone with GO skin [24]. The same authors further improved the fabrication of porous polymeric materials coated with a hybrid GO–CNT layer by electrospinning polycaprolactone solutions onto an active liquid collector made of colloidal suspensions of GO and CNTs in ethanol [25]. The use of 3D graphene-based structures (e.g., open cell foams) is an alternative filtering configuration, which enables achieving a high specific surface area, good mass transfer properties, and low pressure drops thanks to the interconnected macro-porosities of the monolithic structure. Such structures are typically obtained by depositing thin G/GO layers onto inert 3D supports [26]. In a recent detailed review, Sakhadeo et al. discussed the state-of-the-art in washcoating techniques of various polymeric foams by surface treatments and their applications [27]. Chemical vapor deposition (CVD) is a well-known process for GO films preparation [28] and was successfully used to deposit carbon layers onto nickel or copper foams [29,30], evidencing the possibility to deposit high-quality graphene layers on surfaces of different shapes.

The coating of 3D porous structures by CVD involves complex and expensive high-temperature vacuum processes, which may be difficult to be scaled at large production volumes, at the present time [29]. In this view, the activation of inert open cellular supports by slurry coating deposition of GO dispersions may be a good compromise between cost, time, and effectiveness. In this regard, Fenner et al. reported an inexpensive and simple approach to GO deposition onto PU foams; samples with hydrophobic and oleophilic characteristics were obtained and tested for oil adsorption applications [31–33]. Furthermore, a similar approach was applied to coat polymeric sponges with rGO; the samples were then used to adsorb different kinds of organic liquids selectively [32]. Sanati et al. developed a facile and cost-effective method for the production of electrodes for electrochemical applications. The foams were squeezed and immersed into a highly concentrated GO suspension. Accordingly, after coating the polyurethane foam with graphene oxide (GO), boiling ascorbic acid was used for GO reduction [26]. Hodlur et al. demonstrated the production of

highly compressible conducting composites based on graphene layers assembled onto the surface of PU foams to be used as pressure sensors [34]. Similarly, Boland et al. followed a similar procedure for the development of 3D matrices with compressive strain, pressure, and impact sensing properties [35].

While research evidence of GO/rGO deposition onto open cell foams is available in the literature [36], at the present time there is a lack of knowledge regarding the possibility to use GO-activated foams for the water softening process. Given this scenario, in this work, a novel approach to the management of water hardness was investigated, based on the combination of GO and open cellular matrices. In particular, PU open cell foams were activated towards the adsorption of divalent ions by the deposition of thin GO layers. The dip–squeeze washcoating process was selected as the deposition methodology of choice, and the GO load was monitored and tuned by means of multiple depositions. The as-prepared samples were effectively tested in the water softening process, and the performance of the system was evaluated by water titration.

## 2. Materials and Methods

### 2.1. Washcoat Deposition and Characterization

Polyurethane (PU) open cell foams (density of  $0.034 \text{ g}\cdot\text{cm}^{-3}$ ) with a nominal pore density of 60 pores per inch (PPI) were supplied by Modulor GmbH (Berlin, Germany); the bare polymeric support is labelled as F60 in the following. The morphological properties of the bare supports were assessed by optical microscopy (SZ-CTV microscope by Olympus (Tokyo, Japan)). The images of the as-received PU foam were used to carry out a complete morphological characterization of the bare support; accordingly, the cell size, strut size, and strut shape were determined by image processing. Based on these results, the geometric surface area per unit volume (GSA,  $\text{m}^{-1}$ ) and the porosity ( $\epsilon$ ) were determined using correlations reported in the literature [37]. A resume of the geometrical properties of the support is reported in Table 1. The foams were cut in form of cylinders, with diameter and height equal to 25 mm and 50 mm, respectively. Prior to the washcoating process, the foams were washed in deionized water using ultrasound and dried at room temperature.

**Table 1.** Resume of the geometrical properties of the commercial polyurethane open cell foams (F). The number in the sample label indicates the PPI.

Sample name	F60
Bulk material	Polyurethane
Support type	Open cell foam
Cell diameter [ $\mu\text{m}$ ]	$610 \pm 40$
Strut size [ $\mu\text{m}$ ]	$64 \pm 8$
Strut shape	Triangular
Porosity ( $\epsilon$ ) [-]	0.909
Geometric surface area [ $\text{m}^{-1}$ ]	4500

A commercial dispersion of graphene oxide sheets in water (0.4 wt%, supplied by Graphenea Inc. (Pais Vasco, Spain)) was used as a precursor for the coating of PU foams. According to the supplier specification, the elemental composition of GO was as follows: carbon: 49–56%, hydrogen: 1–2%, nitrogen: 0–1%, sulfur: 2–3%, oxygen: 41–50%. The share single layer was >95%, the XY dimension (lateral) was <10  $\mu\text{m}$ , and the thickness (Z dimension) was in the 0.8–1 nm range.

Based on experimental procedures reported in the literature [26,38], the dip–squeeze coating method was chosen. In a typical procedure, the sample was dipped by hand in the GO slurry, aiming at filling the open porosity of the foam. Then, the PU foam was squeezed in order to remove the excess slurry, exploiting the flexibility of the polyurethane material. After the wet coating deposition, the samples were dried for 20 h in a pre-heated ventilated oven, at 45 °C. In the following, the washcoated PU foam is labelled as GO/F60.

In order to characterize the washcoating process, the solid GO load was measured by weighing the samples before and after each deposition using the AS220.R2 model balance (Radwag). The final solid GO washcoat load [wt%] was calculated according to (1)

$$\text{Washcoat load} = \frac{m_{\text{GO}}}{m_{\text{GO}} + m_{\text{foam}}} \cdot 100 \quad (1)$$

where  $m_{\text{GO}}$  [g] and  $m_{\text{foam}}$  [g] correspond to the masses of the deposited GO and of the bare PU foam, respectively. The procedure was repeated up to three times, and the samples were weighed after each deposition to monitor the washcoat load evolution.

In a similar way, the adsorbing medium content was assessed by calculating the GO mass per foam unit volume, according to (2)

$$\text{GO inventory} \left[ \frac{\text{g}}{\text{cm}^3} \right] = \frac{m_{\text{GO}}}{V_{\text{filter}}} \quad (2)$$

where  $m_{\text{GO}}$  [g] is the mass of the deposited GO, and  $V_{\text{filter}}$  [cm<sup>3</sup>] is the volume of the PU foam. The GO inventory parameter was then used for the comparison of the adsorbing performances of the PU foams with different GO washcoat loads.

According to procedures reported in the literature [39], the washcoat adhesion was evaluated by sonication for 30 min in a water bath at room temperature (Labsonic LBS1 instrument by FALC (Faenza, Italy)). Washcoat detachment was measured by weighing the samples before and after the test.

A detailed characterization of the morphology of the washcoated samples was carried out by scanning electron microscope (SEM) analysis (EVO 50 EP by Carl Zeiss AG, (Oberkochen, Germany)) using an accelerating voltage of 20 kV, a maximum current probe of 100 pA, and a pressure in the range of  $4 \cdot 10^{-4}$ – $6 \cdot 10^{-4}$  Pa.

## 2.2. Water Softening Tests

A set of experiments was performed in order to assess the performance of the GO-coated PU foams in water softening. A schematic representation of the experimental setup is reported in Figure 1.

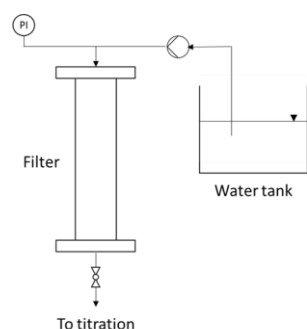


**Figure 1.** Schematic representation of the experimental setup.

In a typical procedure, GO-coated foams, characterized by a certain total volume ( $V_{\text{foam}}$ ), were loaded in a poly(methyl methacrylate) cylinder (20 mm internal diameter and 150 mm height), and water was fed by means of a pump (SPM model by Sankyo (Tokyo, Japan), rated at 6 bar and  $130 \text{ mL} \cdot \text{min}^{-1}$  nominal flow rate). A manometer was mounted on the water feed line to monitor the presence of pressure drops under the water flow; no pressure drops were detected in all the tested configurations.

Before the softening test, a pre-conditioning step was performed, in line with a similar procedure reported in the literature [20]. Accordingly, an aqueous NaCl solution ( $0.1 \text{ g} \cdot \text{mL}^{-1}$ ) was fed to the filter using the same operating conditions as those used in the softening test (i.e., same pump and same flow rate,  $V_{\text{NaCl,sol}}/V_{\text{foam}} = 1$ ).

The softening test was performed using tap water (nominal hardness of inlet water in the 190–270  $\text{mg}_{\text{Ca}^{2+},\text{eq}} \cdot \text{L}^{-1}$  range). The total volume of water to be filtered was calculated according to the quantity of GO deposited onto the foam support; the ratio between total filtered water and GO mass was set to  $0.53 \text{ mL}_{\text{H}_2\text{O}} \cdot \text{mg}_{\text{GO}}^{-1}$ . The outlet water stream was sampled and divided into several batches with fixed volumes (50 mL each).

The total hardness (i.e., the concentration of dissolved  $\text{Ca}^{2+}$  and  $\text{Mg}^{2+}$  ions) was measured by titrating water with ethylenediaminetetraacetic acid (EDTA). In a typical experiment, 20 mL of water was poured in a glass flask. Then, 2 mL of ammonia buffer solution (Idrimer Erba Solution B by Carlo Erba, (Cornaredo, Italy)) was added, together with 1 mg of Eriochrome Black-T indicator (EBT, pure, supplied by Acros Organics, (Geel, Belgium)), thus obtaining the typical purple/wine color solution. The titration was performed by adding the EDTA solution ( $0.01 \text{ mol} \cdot \text{L}^{-1}$ , supplied by Carlo Erba) dropwise using a graduated burette, until the solution changed its color to blue. According to the measured volume of EDTA solution and to its concentration, the effective concentration of  $\text{Mg}^{2+}$  and  $\text{Ca}^{2+}$  was determined.

The overall softening performance of the system was evaluated by calculating the cumulative specific ion adsorption and the cumulative softening efficiency. The first parameter is defined as (3)

$$\text{Cumulative specific ion adsorption} = \frac{\sum_i^{\text{H}_2\text{O},\text{tot}} (C_{\text{Ca},0} - C_{\text{Ca},\text{out},i}) V_i}{m_{\text{GO}}} \quad (3)$$

where  $C_{\text{Ca},0}$  [ $\text{mg} \cdot \text{mL}^{-1}$ ] and  $C_{\text{Ca},\text{out},i}$  [ $\text{mg} \cdot \text{mL}^{-1}$ ] are the equivalent concentrations of calcium carbonate obtained by titration, representing the concentration of divalent ions (i.e.,  $\text{Mg}^{2+}$  and  $\text{Ca}^{2+}$ ) in the inlet and in the  $i$ -th outlet filtered volume ( $V_i$  [mL]), respectively, and  $m_{\text{GO}}$  [g] corresponds to the total mass of deposited GO onto the PU foam surface. The same quantities were used to calculate the cumulative softening efficiency according to (4)

$$\text{Cumulative efficiency} = \frac{\sum_i^{\text{H}_2\text{O},\text{tot}} (C_{\text{Ca},0} - C_{\text{Ca},\text{out},i}) V_i}{\sum_i^{\text{H}_2\text{O},\text{tot}} C_{\text{Ca},0} \cdot V_i} \cdot 100 \quad (4)$$

In all cases, the equivalent concentrations (i.e.,  $C_{\text{Ca},0}$  and  $C_{\text{Ca},\text{out},i}$ ) were obtained by the titration measurements, given the water volume of each sample. The reliability of the total hardness measurement by water titration was validated by an independent analysis performed on the softened water by ICP-OES (OPTIMA 7000 DV spectrometer by Perkin Elmer).

### 3. Results

#### 3.1. Graphene Deposition and Washcoat Characterization

The washcoat load was determined according to (1) and to the experimental procedure reported in Section 2.1; the results are reported in Figure 2, as a function of the number of consecutive depositions.

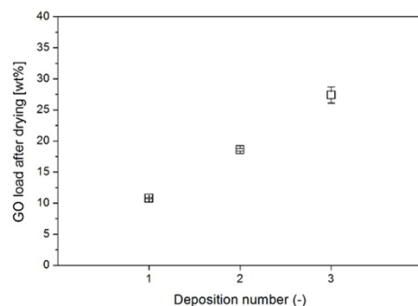


**Figure 2.** Average GO washcoat load as a function of the number of consecutive depositions (the standard deviation is the result of four replicated experiments).

The GO washcoat load increased linearly with the number of consecutive depositions. The maximum load after three consecutive depositions reached values in the  $27 \pm 1$  wt% range. In order to have a clear overview of the morphological properties of the deposited GO layer, the results of the scanning electron microscope characterization are reported in Figure 3. For the sake of comparison, a magnification of the bare PU foam is reported in Figure 3a.

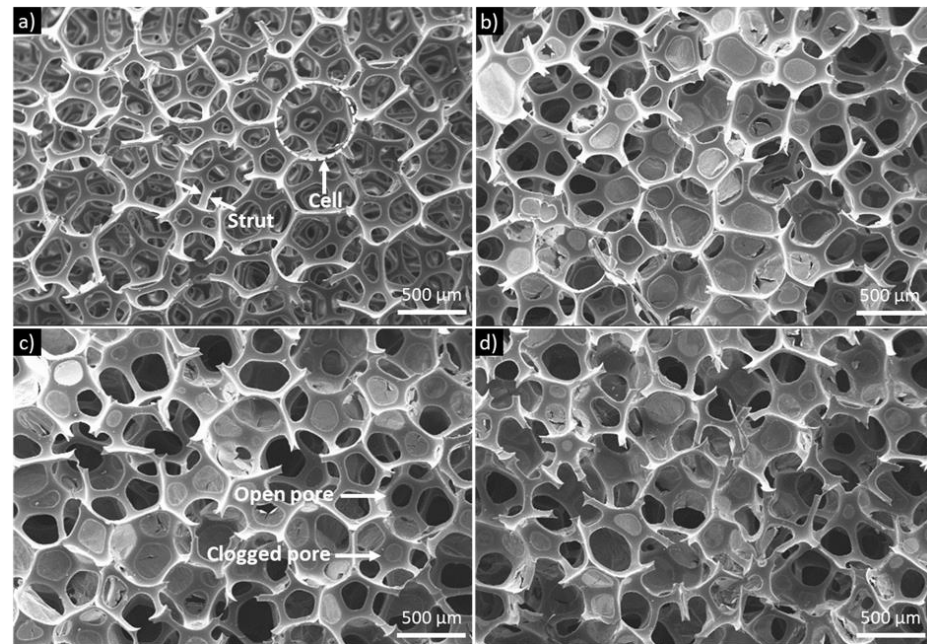


**Figure 3.** SEM images of the bare structured support (a) and of the samples activated by GO washcoat: one deposition (b), two depositions, (c) and three depositions (d).

In all cases, namely, one (Figure 3b), two (Figure 3c), or three (Figure 3d) consecutive depositions, pore clogging phenomena occurred due to the formation of GO layers, as highlighted in Figure 3c.

Pore clogging is typically considered a detrimental phenomenon for washcoated structured supports. In fact, the lack of a strong washcoat-to-substrate interaction typically induces washcoat detachment, when the activated support undergoes mechanical stresses (e.g., sonication). Nevertheless, in the specific case of this work, the self-assembling properties of GO might have provided good adhesion and, in general, mechanical properties to the coating, even far from the PU substrate (i.e., pore windows). Such a behavior may potentially induce a twofold benefit to the overall liquid-to-solid interaction, namely, (i) an increase in terms of GO surface area per unit volume of foam and (ii) a further increase in terms of tortuosity of the flow throughout the porous matrix (with beneficial effects on mass transfer performance).

As reported in Section 2.1, the strength of the deposited washcoat layer was assessed by sonication in water. The results showed average weight losses equal to  $42.3 \pm 6.4$  wt% with respect to the mass of the deposited GO. They were measured for three independent samples, one for each number of consecutive depositions. While the results appeared to indicate a poor washcoat adhesion, it should be noted that such evaluation approach, which is widely accepted for the assessment of the adhesion performance of ceramic coatings onto porous substrates [39], may be oversized for GO-based samples. In this regard, it is worth mentioning that graphene-based materials are typically dispersed in liquid media by means of ultrasound [40,41], which are able to finely disperse the GO aggregates down to monolayer sizes [42]. Moreover, no visible washcoat detachment was detected while feeding water at the testing operating conditions. Based on these considerations, a more

appropriate accelerated stress test procedure should be defined to evaluate the adhesion properties of GO-based coatings onto cellular matrices.

### 3.2. Assessment of the Softening Performance

The results of the cumulative specific ion adsorption and the cumulative softening efficiency are reported in Figures 4a and 4b, respectively, as a function of the specific filtered water volume. Preliminary tests performed on bare PU foams using the same experimental procedure employed for the washcoated samples did not show any adsorbing capacity by the uncoated foam supports.

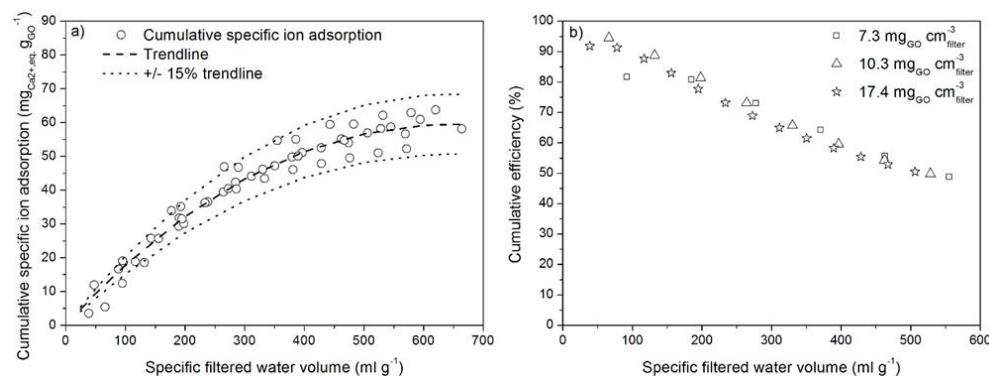


**Figure 4.** Specific cumulative divalent ions adsorption (a) and cumulative efficiency (b) as a function of specific filtered water volume for GO inventories of 7.3, 10.3, and 17.4 mg<sub>GO</sub> per unit volume of foam filter.

As far as the cumulative specific ion adsorption is concerned (Figure 4a), values up to 63 mg<sub>Ca2+,eq</sub>·g<sub>GO</sub><sup>-1</sup> were found, in the specific filtered water volumes range of 600–700 mL<sub>H2O</sub>·g<sub>GO</sub><sup>-1</sup>. Such results were found to be in good agreement with the results obtained by ICP-OES and they are very promising, especially if compared to the state-of-the-art results reported in literature for the use of GO-based materials for water softening. Liang et al. reported an adsorbing capacity up to 50 mg<sub>Ca2+,eq</sub>·g<sub>GO</sub><sup>-1</sup>, which was extrapolated according to experimental results obtained using a single membrane of 5 mg and a total filtered volume of 20 mL [20]. Using an alternative approach, Rocha et al. reported the performance of κ-carrageenan-modified GO, which showed maximum adsorption capacity values of 48 mg<sub>Ca2+,eq</sub>·g<sub>GO</sub><sup>-1</sup> [19]. Such results were obtained by directly contacting hard water and the modified GO, with a contact time of 10 min under similar conditions in terms of specific filtered water volumes.

The specific cumulative ion adsorption tended to plateau values as the specific filtered water volume increased; this trend could have been determined by a progressive saturation of the GO active sites involved in the selective adsorption of Ca<sup>2+</sup>/Mg<sup>2+</sup> ions. The experimental results shared a common trend line and were averagely comprised between ±15% variability lines, demonstrating an overall good reproducibility of the experimental phenomena even under slightly different conditions (i.e., a GO inventory between 7.3 and 17.4 mg<sub>GO</sub>·cm<sup>-3</sup>) and replicated tests.

The softening capacity of the GO/F60 system is likely due to the formation of strong chemical interactions between the oxygen-containing functional groups of GO and Ca<sup>2+</sup>/Mg<sup>2+</sup> ions [20], which results in the adsorption of the divalent metal ions and thus in the softening of hard water. According to this hypothesis, the reduction of the cumulative efficiency with respect to the cumulative filtered water volume (Figure 4b) can be ascribed to a progressive saturation of the oxygen-containing functional groups. The significant variation of GO load values (i.e., from 7.3 to 17.4 mg<sub>GO</sub>·cm<sup>3</sup><sub>filter</sub>) did not seem to have any relevant effect on the cumulative efficiency; this could be qualitatively associated with an overall good utilization of the GO layer, with the absence of relevant limitations to mass transfer phenomena.

#### 4. Conclusions

In this short communication, the activation of 60 PPI PU open cell foams by the deposition of thin GO washcoat layers was investigated as a promising approach to the management of water hardness. The following points represent the most significant achievements of the reported experimental investigation:

The functionalization of the PU foam surface was achieved by implementing the facile and low-cost dip–squeeze coating procedure, which demonstrated good reproducibility (i.e., small standard deviation values of replicated tests for an increasing number of consecutive depositions).

The deposited GO layers were found to be effective in the reduction of  $\text{Ca}^{2+}/\text{Mg}^{2+}$  ion concentrations during the filtration process. Values up to  $63 \text{ mg}_{\text{Ca}^{2+},\text{eq}} \cdot \text{g}_{\text{GO}}^{-1}$  were obtained in the specific filtered water volumes range of 600–700  $\text{mL}_{\text{H}_2\text{O}} \cdot \text{g}_{\text{GO}}^{-1}$ .

The results in terms of adsorbing capacity displayed a twofold improvement with respect to the current state-of-the-art adsorbing capacity of GO-based softening systems. Firstly, the adsorbing capacity was significantly raised, as a +26% improvement of the maximum adsorption capacity was recorded with respect to literature-reported results (i.e., from  $50 \text{ mg}_{\text{Ca}^{2+},\text{eq}} \cdot \text{g}_{\text{GO}}^{-1}$  (literature) to  $63 \text{ mg}_{\text{Ca}^{2+},\text{eq}} \cdot \text{g}_{\text{GO}}^{-1}$  (this work)). Secondly, such results were obtained using a heterogeneous system characterized by low-pressure drops, which represents a remarkable improvement with respect to the current state-of-the-art GO-based materials (i.e., “slurry-based” and membrane-based systems).

The use of alternative open cellular matrices (e.g., different porosity, additively manufactured) and a thorough experimental campaign focused on the performance-wise optimization of the GO washcoat properties could pave the way to a further improvement of the overall effectiveness of the system.

**Author Contributions:** Conceptualization, R.B. and A.M. (Alessandro Migliavacca); methodology, R.B. and A.M. (Alessandro Migliavacca); formal analysis, A.M. (Alessandro Migliavacca), A.B.P. and S.L.; investigation, R.B. and A.M. (Alessandro Migliavacca); data curation, A.B.P.; writing—original draft preparation, R.B. and A.M. (Alessandro Migliavacca); writing—review and editing, A.B.P., S.L. and A.M. (Alessandro Mansutti); supervision, S.L. and A.M. (Alessandro Mansutti). All authors have read and agreed to the published version of the manuscript.

**Funding:** This research received no external funding.

**Institutional Review Board Statement:** Not applicable.

**Informed Consent Statement:** Not applicable.

**Data Availability Statement:** The data presented in this study are available on request from the corresponding author.

**Conflicts of Interest:** The authors declare no conflict of interest.

#### References

1. Geim, A.K.; Novoselov, K.S. The rise of graphene. *Nat. Mater.* **2007**, *6*, 183–191. [[CrossRef](#)]
2. Allen, M.J.; Tung, V.C.; Kaner, R.B. Honeycomb Carbon: A Review of Graphene. *Chem. Rev.* **2010**, *110*, 132–145. [[CrossRef](#)]
3. Lee, X.J.; Hiew, B.Y.Z.; Lai, K.C.; Lee, L.Y.; Gan, S.; Thangalazhy-Gopakumar, S.; Rigby, S. Review on graphene and its derivatives: Synthesis methods and potential industrial implementation. *J. Taiwan Inst. Chem. Eng.* **2019**, *98*, 163–180. [[CrossRef](#)]
4. Liu, J.; Chen, F.; Yao, Q.; Sun, Y.; Huang, W.; Wang, R.; Yang, B.; Li, W.; Tian, J. Application and prospect of graphene and its composites in wastewater treatment. *Polish J. Environ. Stud.* **2020**, *29*, 3965–3974. [[CrossRef](#)]
5. Anand, A.; Unnikrishnan, B.; Mao, J.-Y.; Lin, H.-J.; Huang, C.-C. Graphene-based nanofiltration membranes for improving salt rejection, water flux and antifouling—A review. *Desalination* **2018**, *429*, 119–133. [[CrossRef](#)]
6. Castelletto, S.; Boretti, A. Advantages, limitations, and future suggestions in studying graphene-based desalination membranes. *RSC Adv.* **2021**, *11*, 7981–8002. [[CrossRef](#)] [[PubMed](#)]
7. Buelke, C.; Alshami, A.; Casler, J.; Lewis, J.; Al-Sayaghi, M.; Hickner, M.A. Graphene oxide membranes for enhancing water purification in terrestrial and space-born applications: State of the art. *Desalination* **2018**, *448*, 113–132. [[CrossRef](#)]
8. Han, Z.-Y.; Huang, L.-J.; Qu, H.-J.; Wang, Y.-X.; Zhang, Z.-J.; Rong, Q.-L.; Sang, Z.-Q.; Wang, Y.; Kipper, M.J.; Tang, J.-G. A review of performance improvement strategies for graphene oxide-based and graphene-based membranes in water treatment. *J. Mater. Sci.* **2021**, *56*, 9545–9574. [[CrossRef](#)]



9. You, Y.; Sahajwalla, V.; Yoshimura, M.; Joshi, R.K. Graphene and graphene oxide for desalination. *Nanoscale* **2016**, *8*, 117–119. [[CrossRef](#)]
10. Alen, S.K.; Nam, S.; Dastgheib, S.A. Recent advances in graphene oxide membranes for gas separation applications. *Int. J. Mol. Sci.* **2019**, *20*, 5609. [[CrossRef](#)] [[PubMed](#)]
11. Kwon, O.; Choi, Y.; Choi, E.; Kim, M.; Woo, Y.C.; Kim, D.W. Fabrication Techniques for Graphene Oxide-Based Molecular Separation Membranes: Towards Industrial Application. *Nanomaterials* **2021**, *11*, 757. [[CrossRef](#)] [[PubMed](#)]
12. RPandey, R.P.; Shukla, G.; Manohar, M.; Shahi, V.K. Graphene oxide based nanohybrid proton exchange membranes for fuel cell applications: An overview. *Adv. Colloid Interface Sci.* **2017**, *240*, 15–30. [[CrossRef](#)] [[PubMed](#)]
13. Migliavacca, A.; Latorrata, S.; Stampino, P.G.; Dotelli, G. Preparation and characterization of graphene oxide based membranes as possible Gas Diffusion Layers for PEM fuel cells with enhanced surface homogeneity. *Mater. Today Proc.* **2017**, *4*, 11594–11607. [[CrossRef](#)]
14. Peressut, A.B.; Latorrata, S.; Stampino, P.G.; Dotelli, G. Development of self-assembling sulfonated graphene oxide membranes as a potential proton conductor. *Mater. Chem. Phys.* **2021**, *257*, 123768. [[CrossRef](#)]
15. Liu, Y. Application of graphene oxide in water treatment. *IOP Conf. Ser. Earth Environ. Sci.* **2017**, *94*, 012060. [[CrossRef](#)]
16. Li, B.; Wang, C.-G.; Surat'Man, N.E.; Loh, X.J.; Li, Z. Microscopically tuning the graphene oxide framework for membrane separations: A review. *Nanoscale Adv.* **2021**, *3*, 5265–5276. [[CrossRef](#)]
17. Wei, Y.; Zhang, Y.; Gao, X.; Ma, Z.; Wang, X.; Gao, C. Multilayered graphene oxide membranes for water treatment: A review. *Carbon N. Y.* **2018**, *139*, 964–981. [[CrossRef](#)]
18. Latorrata, S.; Cristiani, C.; Peressut, A.B.; Brambilla, L.; Bellotto, M.; Dotelli, G.; Finocchio, E.; Stampino, P.G.; Ramis, G. Reduced Graphene Oxide Membranes as Potential Self-Assembling Filter for Wastewater Treatment. *Minerals* **2021**, *11*, 15. [[CrossRef](#)]
19. Rocha, L.S.; Nogueira, J.; Daniel-Da-Silva, A.L.; Marques, P.; Fateixa, S.; Pereira, E.; Trindade, T. Water softening using graphene oxide/biopolymer hybrid nanomaterials. *J. Environ. Chem. Eng.* **2021**, *9*, 105045. [[CrossRef](#)]
20. Liang, J.; Huang, Y.; Zhang, F.; Zhang, Y.; Li, N.; Chen, Y. The use of graphene oxide membranes for the softening of hard water. *Sci. China Technol. Sci.* **2014**, *57*, 284–287. [[CrossRef](#)]
21. Petukhov, D.I.; Kapitanova, O.O.; Eremina, E.A.; Goodilin, E.A. Preparation, chemical features, structure and applications of membrane materials based on graphene oxide. *Mendeleev Commun.* **2021**, *31*, 137–148. [[CrossRef](#)]
22. Yousefi, N.; Lu, X.; Elimelech, M.; Tufenkji, N. Environmental performance of graphene-based 3D macrostructures. *Nat. Nanotechnol.* **2019**, *14*, 107–119. [[CrossRef](#)]
23. Mahalingam, D.K.; Falca, G.; Upadhyya, L.; Abou-Hamad, E.; Batra, N.; Wang, S.; Musteata, V.; da Costa, P.M.; Nunes, S.P. Spray-coated graphene oxide hollow fibers for nanofiltration. *J. Memb. Sci.* **2020**, *606*, 118006. [[CrossRef](#)]
24. Maio, A.; Gammino, M.; Gulino, E.F.; Megna, B.; Fara, P.; Scaffaro, R. Rapid One-Step Fabrication of Graphene Oxide-Decorated Polycaprolactone Three-Dimensional Templates for Water Treatment. *ACS Appl. Polym. Mater.* **2020**, *2*, 4993–5005. [[CrossRef](#)]
25. Scaffaro, R.; Gammino, M.; Maio, A. Wet electrospinning-aided self-assembly of multifunctional GO-CNT@PCL core-shell nanocomposites with spider leg bioinspired hierarchical architectures. *Compos. Sci. Technol.* **2022**, *221*, 109363. [[CrossRef](#)]
26. Sanati, A.; Raeissi, K.; Karimzadeh, F. A cost-effective and green-reduced graphene oxide/polyurethane foam electrode for electrochemical applications. *FlatChem* **2020**, *20*, 100162. [[CrossRef](#)]
27. Sakhadeo, N.N.; Patro, T.U. Exploring the Multifunctional Applications of Surface-Coated Polymeric Foams—A Review. *Ind. Eng. Chem. Res.* **2022**, *61*, 5366–5387. [[CrossRef](#)]
28. Plutnar, J.; Pumera, M.; Sofer, Z. The chemistry of CVD graphene. *J. Mater. Chem. C* **2018**, *6*, 6082–6101. [[CrossRef](#)]
29. Chen, Z.; Ren, W.; Gao, L.; Liu, B.; Pei, S.; Cheng, H.-M. Three-dimensional flexible and conductive interconnected graphene networks grown by chemical vapour deposition. *Nat. Mater.* **2011**, *10*, 424–428. [[CrossRef](#)]
30. Wong, R.; Antoniou, A.; Smet, V. Copper-Graphene Foams: A New High-Performance Material System for Advanced Package-Integrated Cooling Technologies. In Proceedings of the 2021 IEEE 71st Electronic Components and Technology Conference (ECTC), San Diego, CA, USA, 1 June–4 July 2021; pp. 1945–1951. [[CrossRef](#)]
31. BFenner, B.R.; Zimmermann, M.V.; da Silva, M.P.; Zattera, A.J. Comparative analysis among coating methods of flexible polyurethane foams with graphene oxide. *J. Mol. Liq.* **2018**, *271*, 74–79. [[CrossRef](#)]
32. Liu, Y.; Ma, J.; Wu, T.; Wang, X.; Huang, G.; Qiu, H.; Li, Y.; Wang, W.; Gao, J. Cost-effective reduced graphene oxide-coated polyurethane sponge as a highly efficient and reusable oil-absorbent. *ACS Appl. Mater. Interfaces* **2013**, *5*, 10018–10026. [[CrossRef](#)] [[PubMed](#)]
33. Tjandra, R.; Lui, G.; Veilleux, A.; Broughton, J.; Chiu, G.; Yu, A. Introduction of an enhanced binding of reduced graphene oxide to polyurethane sponge for oil absorption. *Ind. Eng. Chem. Res.* **2015**, *54*, 3657–3663. [[CrossRef](#)]
34. Hodlur, R.; Rabinal, M. Self assembled graphene layers on polyurethane foam as a highly pressure sensitive conducting composite. *Compos. Sci. Technol.* **2014**, *90*, 160–165. [[CrossRef](#)]
35. Boland, C.S.; Khan, U.; Binions, M.; Barwich, S.; Boland, J.B.; Weaire, D.; Coleman, J.N. Graphene-coated polymer foams as tuneable impact sensors. *Nanoscale* **2018**, *10*, 5366–5375. [[CrossRef](#)]
36. Ba, H.; Truong-Phuoc, L.; Romero, T.; Sutter, C.; Nhut, J.-M.; Schlatter, G.; Giambastiani, G.; Pham-Huu, C. Lightweight, few-layer graphene composites with improved electro-thermal properties as efficient heating devices for de-icing applications. *Carbon* **2021**, *182*, 655–668. [[CrossRef](#)]

37. Ambrosetti, M.; Bracconi, M.; Groppi, G.; Tronconi, E. Analytical Geometrical Model of Open Cell Foams with Detailed Description of Strut-Node Intersection. *Chem. Ing. Tech.* **2017**, *89*, 915–925. [[CrossRef](#)]
38. Balzarotti, R.; Bisaccia, A.; Tripi, M.C.; Ambrosetti, M.; Groppi, G.; Tronconi, E. Production and characterization of copper periodic open cellular structures made by 3D printing-replica technique. *J. Adv. Manuf. Process.* **2020**, *2*, e10068. [[CrossRef](#)]
39. Balzarotti, R.; Fratolocchi, L.; Latorrata, S.; Finocchio, E.; Cristiani, C. Effective Ce-based catalysts deposition on ceramic open cell foams. *Appl. Catal. A Gen.* **2019**, *584*, 117089. [[CrossRef](#)]
40. Zhang, W.; He, W.; Jing, X. Preparation of a stable graphene dispersion with high concentration by ultrasound. *J. Phys. Chem. B* **2010**, *114*, 10368–10373. [[CrossRef](#)]
41. Zhang, B.; Chen, T. Study of ultrasonic dispersion of graphene nanoplatelets. *Materials* **2019**, *12*, 1757. [[CrossRef](#)]
42. Tyurnina, A.V.; Tzanakis, I.; Morton, J.; Mi, J.; Porfyrakis, K.; Maciejewska, B.M.; Grobert, N.; Eskin, D.G. Ultrasonic exfoliation of graphene in water: A key parameter study. *Carbon* **2020**, *168*, 737–747. [[CrossRef](#)]

**Disclaimer/Publisher's Note:** The statements, opinions and data contained in all publications are solely those of the individual author(s) and contributor(s) and not of MDPI and/or the editor(s). MDPI and/or the editor(s) disclaim responsibility for any injury to people or property resulting from any ideas, methods, instructions or products referred to in the content.